

***Ab initio* calculations of quasiparticle band structure in correlated systems: LDA++ approach**

A. I. Lichtenstein

Forschungszentrum Jülich, D-52428 Jülich, Germany

M. I. Katsnelson

Institute of Metal Physics, Ekaterinburg 620219, Russia

(Received 11 July 1997)

We discuss a general approach to a realistic theory of the electronic structure in materials containing correlated d or f electrons. The main feature of this approach is the taking into account of the energy dependence of the electron self-energy with the momentum dependence being neglected (local approximation). It allows us to consider such correlation effects as the non-Fermi-step form of the distribution function, the enhancement of the effective mass including Kondo resonances, the appearance of the satellites in the electron spectra, etc. To specify the form of the self-energy, it is useful to distinguish (according to the ratio of the on-site Coulomb energy U to the bandwidth W) three regimes—strong, moderate, and weak correlations. In the case of strong interactions ($U/W > 1$ —rare-earth system) the Hubbard-I approach is the most suitable. Starting from an exact atomic Green function with the constrained density matrix $n_{mm'}$, the band-structure problem is formulated as the functional problem on $n_{mm'}$ for f electrons and the standard local-density-approximation functional for delocalized electrons. In the case of moderate correlations ($U/W \sim 1$ —metal-insulator regime, Kondo systems) we start from the $d = \infty$ dynamical mean-field iterative perturbation scheme of Kotliar and co-workers and also make use of our multiband atomic Green function for constrained $n_{mm'}$. Finally for the weak interactions ($U/W < 1$ —transition metals) the self-consistent diagrammatic fluctuation-exchange approach of Bickers and Scalapino is generalized to the realistic multiband case. We present two-band, two-dimensional model calculations for all three regimes. A realistic calculation in the Hubbard-I scheme with the exact solution of the on-site multielectron problem for $f(d)$ shells was performed for mixed-valence $4f$ compound TmSe, and for the classical Mott insulator NiO. [S0163-1829(98)05112-1]

I. INTRODUCTION

A general accurate description of the electronic structure of materials with correlated electrons has yet to be developed. Such materials include the high- T_c and colossal magnetoresistance (CMR) materials, as well as the mixed-valence and heavy-fermion compounds. All these systems demonstrate essentially many-particle (correlation) features in their excitation spectrum and ground-state properties, the usual language of one-electron band theory being inadequate to describe such features even qualitatively: e.g., the problem of Mott insulators, the heavy-fermion behavior in some rare-earth compounds, satellites and “midgap states” in electron spectra, etc. (see, e.g., recent reviews¹⁻⁴). Such effects as the metal-insulator transition, Kondo effect, and others, which help us to understand the basic physics in these strongly correlated materials, is usually considered in the framework of simplified models such as the Hubbard model, Anderson model, s - f exchange model, and other correlation models. Nevertheless, the complexity of the crystals containing 10–15 different atoms per unit cell, and the interactions between electronic and lattice degrees of freedom demand a more detailed investigation of the energy bands in such systems. The only general first-principles approaches that take into account in practice specific peculiarities of the electronic structure in real compounds are those based on the density-functional theory (DFT).⁵ The vast majority of practical DFT applications today are based on the local-density approximation (LDA), which treats the exchange-correlation (XC) part

of an effective single-particle DFT potential as a density-dependent XC potential, taken from the exact quantum Monte Carlo (QMC) results for the homogeneous electron gas. There are many successes but also some failures of the LDA approach,⁶ related to the simple fact that, in cases where some portion of the electronic structure is better described in terms of atomlike electronic states, the homogeneous electron gas approximation is not a good starting point. Another limitation of LDA theory is that it is only a ground-state scheme and the one-particle band structure itself has, generally speaking, no proper meaning. Recently the time-dependent (TD-LDA) approach has been applied for calculations of excitation energies,^{7,8} but the TD-LDA effective potential is not known as well as the LDA one. On the other hand, exact QMC calculations for real materials which have tedious first-principles Hartree-Fock band structure as zero-order approximations is still a challenging problem of solid state theory.⁹⁻¹¹

In this situation it is useful to have a simple and accurate scheme that could still capture the most important properties of real electronic structure and at the same time could take into account the most important correlation effects. One of the first successful approaches in this line was the GW approximation¹² for quasiparticle spectra in solids with the self-energy related to a “bare” Green function (G) and a screened Coulomb interaction (W). Self-consistent GW calculations basing on the LDA band structure give a much better description of a Mott insulator such as NiO than does pure LDA.¹³ Still, the nonlocal Coulomb interactions make

such type of calculations really time consuming. For the purpose of only band-structure investigations one could use a simplified time-independent GW scheme or the so-called screen-exchange LDA approach.^{14,15} The latter approach has some of the same drawbacks as the Hartree-Fock approximation and did not prove suitable for strongly correlated systems. A different way to incorporate some correlation effect in the systems with localized d or f states was successfully done in the so-called LDA+ U method.¹⁶ In this case a simple mean-field Hubbard-like term is added to LDA functionals for the localized state and care must be taken for correction of the LDA double counting.¹⁷ This approach can also be viewed as a density-functional theory, since the U terms that depend on occupation number for localized electrons is a function of the total density. So one just uses the LDA functional for delocalized electrons and improved LDA+ U functional for localized atomiclike states. This approach produces a more reliable description of the electronic and crystal structure of correlated materials with charge, spin, and orbital ordering than does the LSDA scheme.¹⁸ But the LDA+ U scheme, as well as the approach based on the so-called self-interaction corrections (SIC),¹⁹ has one intrinsic shortcoming related with a mean-field approximation. It is well known (see, e.g., Refs. 20 and 21) that the most interesting correlation effects in quasiparticle spectra, such as the mass enhancement, damping, and the difference of the distribution function from the ‘‘Fermi step’’ are connected with the energy dependence of the self-energy $\Sigma(\omega)$, so one needs to generalize the LDA+ U approach to include dynamical effects. Such a scheme we would like to call LDA++.²² One can mention a few successful attempts in this direction: quasiparticle (QP) band-structure calculation of Fe, Co, and Ni (Refs. 23–25) as well as a heavy fermion system^{26,27} using simplest second-order local approximation for the self-energy; the QP-band structure of NiO (Refs. 28 and 29) using the three-body Faddeev approximation; the random-phase-approximation-like approach for high-temperature superconductors (HTSC) (Ref. 30) and non-crossing approximations (NCA’s) for Kondo systems.³¹ At the same time, a criterion for the applicability of specific approximations used in these works was not clear.

In this paper we propose a general scheme for LDA++ band-structure calculations for real materials with a different strength of electronic correlations. It is not very efficient from the computational point of view (as well as not very reasonable from the purely theoretical one) to use the only LDA++ scheme for materials with different electron-electron interactions. In accordance with the ratio of average on-site Coulomb parameter U to the relevant valence-band width W , it is useful to distinguish three regimes of weak, moderate, and strong correlations.

For the simplest case of weak correlations ($U/W < 1$ —transition metals) we could use the self-consistent diagrammatic approach. The most convenient way is the conserving fluctuation exchange (FLEX) approximation³² and we will use the multiband generalizations for the LDA++ weak-correlation scheme. The characteristic feature of this renormalized band regime is that no additional states appear in the electronic structure due to interactions or, more exactly, there is one-to-one correspondence of quasiparticle states with and without interaction.

Roughly speaking, the shape of energy bands may be changed but there is no band splitting, or presence of additional bands. The most interesting physical phenomena in this case are the renormalization of the effective masses, flattening of Van Hove singularities, etc.

In the case of very strong interactions ($U/W > 1$ —rare-earth system) we will start with the exact atomic Green function for f states and use the Hubbard-I approximation (HIA) (Ref. 33) to analyze the spectrum of f systems. This approach also may be applied to such d systems as Mott insulators with very narrow d bands. For this situation the electronic structure of solids will combine the many-body structure of $f(d)$ ions and broad bands from delocalized electrons. In this case such phenomena as multiplet structure, satellites in photoelectron spectra, the narrowing of the electron bands depending on the magnetic ordering, etc. are the subjects of main interests.

In the most difficult case of strongly correlated physics ($U/W \sim 1$ —metal-insulator transition regime or Kondo systems) we will use the interpolation scheme based on dynamical mean-field theory (DMFT).³ In this situation we will have a three-peak structure from a single correlated band, consisting of upper and lower Hubbard bands and Kondo resonance near the Fermi energy. Such a scheme is the most accurate, but also the most time consuming, and it is difficult to make a self-consistent calculation for a large system. The other point of view of the different LDA++ schemes could be related to the different energy scales for the spectrum of correlated materials: if one is interested in the large energy scale, the HIA approximation is sufficient for spectroscopic purposes. If we wish to describe the low-energy scale of a system like doped Mott insulators or mixed valence systems, then the DMFT approach is the most appropriate.

The common feature of all LDA++ methods is the matrix form of self-energy since electron-electron correlations can be diagonalized neither in band index n nor in orbital indices lm . This peculiarity of multiband Hubbard interactions is normally ignored and only a few examples of matrix self-energy exist for a transition metal with the LDA second-order perturbation scheme.^{23,25} transition-metal oxides within the three-body Faddeev approximation,²⁹ and for the two-band Hubbard model, investigation of orbital and magnetic instabilities.³⁴

This paper is organized as follows. In Sec. II we will give a general description of different correlation schemes to the dynamical mean-field band-structure calculations. The simple two-band model (Sec. III) will illustrate in practice all LDA++ methods. In Sec. IV we will give an example of first-principles calculations of mixed-valence system TmSe and classical Mott insulator NiO within Hubbard-I approximation to LDA++. Finally we summarize our results in Sec. V.

II. LDA++ METHODS

The Kohn-Sham energies of one-particle LDA states cannot be considered as the quasiparticle energies in the sense of many-particle theory (see, e.g., Refs. 20 and 21). In the LDA++ approach they considered only as the bare energies, which are supposed to be renormalized by the correlation effects. Of course they contain already some part of the correlation effects but only those that may be considered in the

local-density approximation. The most important “rest” in a strongly correlated system is the correlations of the Hubbard type³³ due to the intrasite Coulomb repulsion. Therefore our starting point is the same as in the LDA+ U approach. We proceed with the Hamiltonian

$$H = \sum_{ij\{\sigma\}\{m\}} t_{m_1 m_2}^{ij} c_{im_1 \sigma}^+ c_{jm_2 \sigma} + \frac{1}{2} \sum_{i\{\sigma m\}} U^i c_{m_1 m_2 m_1' m_2'}^+ c_{im_1 \sigma}^+ c_{im_2 \sigma'}^+ c_{im_2 \sigma'} c_{im_1' \sigma}, \quad (1)$$

where (i, j) represents different crystal sites, $\{m\}$ labels different orbitals, and the $\{\sigma\}$ are spin indices. Coulomb matrix elements are defined in the usual way:

$$U_{m_1 m_2 m_1' m_2'} = \int \int d\mathbf{r} d\mathbf{r}' \psi_{m_1}^*(\mathbf{r}) \psi_{m_2}^*(\mathbf{r}') \times V_{ee}(\mathbf{r} - \mathbf{r}') \psi_{m_1'}(\mathbf{r}) \psi_{m_2'}(\mathbf{r}'); \quad (2)$$

here $V_{ee}(\mathbf{r} - \mathbf{r}')$ is the screened Coulomb interactions and $\psi_m(\mathbf{r})$ are localized on-site basis functions (the site index being suppressed).

In this case all the orbitals are assumed to belong to the correlated set, while in real materials like high- T_c compounds (e.g., YBa₂Cu₃O₇) we may define as a first approximation only the 3d orbitals as correlated ones. Therefore it is more reasonable to rewrite Eq. (1) in the form of LDA+ U Hamiltonian:

$$H = H_{dc}^{\text{LDA}} + \frac{1}{2} \sum_{i\{\sigma m\}} U^i c_{m_1 m_2 m_1' m_2'}^+ c_{im_1 \sigma}^+ c_{im_2 \sigma'}^+ c_{im_2 \sigma'} c_{im_1' \sigma}. \quad (3)$$

Note that index i in the second sum of Eq. (3) is running only for correlated sites, and orbital indices $\{m\}$ only for correlated states (e.g., 3d or 4f) while the first LDA term,

$$H_{dc}^{\text{LDA}} = \sum_{ij\{\sigma m\}} h_{m_1 m_2 \sigma}^{ij} c_{im_1 \sigma}^+ c_{jm_2 \sigma} - E_{dc},$$

contains all sites and orbitals in the unit cell. Here $h_{m_1 m_2 \sigma}^{ij}$ are the one-particle Hamiltonian parameters in the (spin-polarized) LDA, E_{dc} is the double counting correction for average Coulomb interactions in L(S)DA:¹⁷

$$E_{dc} = \frac{1}{2} \bar{U} n_d (1 - n_d) - \frac{1}{2} \bar{J} [n_{d\uparrow} (1 - n_{d\uparrow}) + n_{d\downarrow} (1 - n_{d\downarrow})]$$

with \bar{U} and \bar{J} being average Coulomb and exchange interactions, and $n_d = n_{d\uparrow} + n_{d\downarrow}$ is the total number of correlated $d(f)$ electrons.

One nontrivial problem is to find an efficient way to compute the one electron Hamiltonian h^{LDA} in a minimal orthogonal basis set. Orthogonality of the basis functions is required for the use of the second quantization form of the effective Hamiltonian [(Eq. (1))]. Since the many-body (U) part of the problem is an order of magnitude more time consuming than the LDA one, we need to use a minimal basis set and integrate out all high-energy degrees of freedom (out of the $\pm U$ range). One of the best LDA methods for such a scheme is the linear muffin-tin orbital (LMTO) method,³⁵ which could give the orthogonal down-folded one-electron

tight-binding Hamiltonian. In this case LDA calculations were corrected for double counting, produce the first-principles hopping t_{ij} in the many-body Hamiltonian.

Now we can describe methods for efficient calculations of quasiparticle (QP) spectra for the LDA+ U Hamiltonian. In this sense our approach is no longer density-functional theory and one could benefit from, possibly using the information on QP-band structure as compared with different “excitation” experiments.

A. Multiband FLEX

In this section we generalize the FLEX equations³² for the purpose of the multiband LDA++ scheme. We will not take into account a momentum \mathbf{q} dependence of the self-energy, although in the FLEX approximation it is straightforward to include it in all the following formulas. The numerical computation of the (\mathbf{q}, ω) -dependent self-energy is time consuming in the multiband case.^{36,37} To unify the approximations for all our LDA++ schemes we will not include explicitly the \mathbf{q} dependence in the FLEX formalism.

First of all, one needs to symmetrize the bare vertex matrix U over different fluctuation channels: the particle-hole (density- U^d and magnetic- U^m) and particle-particle (singlet- U^s and triplet- U^t) vertex matrices:

$$U_{m_1 m_1' m_2 m_2'}^d = 2U_{m_1 m_2 m_1' m_2'} - U_{m_1 m_2 m_2' m_1'},$$

$$U_{m_1 m_1' m_2 m_2'}^m = -U_{m_1 m_2 m_2' m_1'},$$

$$U_{m_1 m_1' m_2 m_2'}^s = \frac{1}{2} (U_{m_1 m_1' m_2 m_2'} + U_{m_1 m_1' m_2' m_2}),$$

$$U_{m_1 m_1' m_2 m_2'}^t = \frac{1}{2} (U_{m_1 m_1' m_2 m_2'} - U_{m_1 m_1' m_2' m_2}).$$

The one-electron Green function is defined through the following equation:

$$G_{mm' \sigma}^{-1}(i\omega_n) = (i\omega_n + \mu) \delta_{mm' \sigma} - h_{mm' \sigma} - \sum_{mm' \sigma}^{\text{HF}} - \sum_{mm' \sigma}(i\omega_n);$$

here μ is chemical potential, $\omega_n = (2n + 1)/\beta$ are Matsubara frequencies, and $\beta = 1/k_B T$ is the inverse temperature. The frequency-independent Hartree Fock part is

$$\sum_{mm' \sigma}^{\text{HF}} = \sum_{m_1 m_2} \left(U_{mm_1 m_1' m_2} \sum_{\sigma'} n_{m_1 m_2}^{\sigma'} - U_{mm_1 m_2 m_1'} n_{m_1 m_2}^{\sigma} \right) \quad (4)$$

and corresponds to the rotationally invariant LDA+ U method.³⁸

It is useful to write the multiband FLEX equations using matrix-vector notation for different Coulomb matrix vertices and the vector Green function. We will use a combined index: $\alpha = \{m, m'\}$ and define the vector Green function as well as matrix interactions in the following way:

$$\mathbf{G} \equiv \{G_{\alpha\beta}\}, \quad \hat{U} = \{U_{\alpha\alpha'}\}.$$

For simplicity we first write equations for nonpolarized spin states and omit the spin indices. In this case the Hartree-Fock approximation, Eq. (4), can be rewritten in the form of a matrix-vector product only with the density Coulomb interaction:

$$\Sigma^{\text{HF}} = \hat{U}^d * \mathbf{n},$$

where the occupation matrix is defined as

$$n_{\alpha} \equiv n_{mm'}^{\sigma} = \langle c_{m\sigma}^{\dagger} c_{m'\sigma} \rangle = \frac{1}{\beta} \sum_{\omega_n} G_{m'm}(i\omega_n) + \frac{1}{2} \delta_{mm'}.$$

Using the single-site Hubbard interactions one obtains a local form of FLEX equations in the frequency (ω)-time (τ) space. It is very efficient to use fast-Fourier transforms with periodic boundary condition.³⁹ Time-frequency spaces are connected by

$$\mathbf{G}(i\omega_n) = \int_0^{\beta} e^{i\omega_n\tau} \mathbf{G}(\tau) d\tau,$$

$$\mathbf{G}(\tau) = \frac{1}{\beta} \sum_{\omega_n} e^{-i\omega_n\tau} \mathbf{G}(i\omega_n).$$

We will try to keep this dual (ω - τ) notation to stress the numerical implementation of this LDA++ scheme. We write the approximation for self-energy in the GW -like form:

$$\Sigma(\tau) = \hat{W}(\tau) * \mathbf{G}(\tau), \quad (5)$$

where symmetrized fluctuation $W(i\omega)$ -potential is defined as

$$W_{m_1 m_2 m'_1 m'_2} = V_{m_1 m'_1, m'_2 m_2}$$

and total fluctuation potential consists of the second-order term, as well as particle-hole and particle-particle contributions:

$$\hat{V}(i\omega) = \hat{V}_2(i\omega) + \hat{V}_{\text{ph}}(i\omega) - \hat{V}_{\text{pp}}(-i\omega).$$

All these contributions can be expressed in terms of bare (D_0, M_0, S_0, T_0) and renormalized (D, M, S, T) channel propagators. The second-order potential for the nonmagnetic case is

$$\hat{V}_2(i\omega) = \hat{U} * \hat{D}_0(i\omega) * \hat{U}^d \quad (6)$$

while the particle-hole potential is expressed through the density and magnetic fluctuations:

$$\hat{V}_{\text{ph}}(i\omega) = \frac{1}{2} \hat{U}^d * [\hat{D}(i\omega) - \hat{D}_0(i\omega)] * \hat{U}^d + \frac{3}{2} \hat{U}^m * [\hat{M}(i\omega) - \hat{M}_0(i\omega)] * \hat{U}^m.$$

Finally the particle-particle contribution to the fluctuation-exchange potential is

$$\hat{V}_{\text{pp}}(i\omega) = \hat{U}^s * [\hat{S}(i\omega) - \hat{S}_0(i\omega)] * \hat{U}^s + 3 \hat{U}^t * [\hat{T}(i\omega) - \hat{T}_0(i\omega)] * \hat{U}^t.$$

If one defines the particle-hole (χ) and particle-particle (π) ‘‘empty loop’’ susceptibilities,

$$\chi_{m_1 m_2 m_3 m_4}(\tau) = -G_{m_4 m_1}(-\tau) * G_{m_2 m_3}(\tau), \quad (7)$$

$$\pi_{m_1 m_2 m_3 m_4}(\tau) = G_{m_1 m_4}(\tau) * G_{m_2 m_3}(\tau),$$

we can write with this notations for susceptibilities the bare channel propagator matrices in the following form for the density and magnetic part,

$$\hat{D}_0 = \hat{M}_0 = \hat{\chi},$$

and for singlet and triplet bare propagators,

$$S_{m_1 m_2 m_3 m_4}^0 = \frac{1}{2} (\pi_{m_1 m_2 m_3 m_4} + \pi_{m_1 m_2 m_4 m_3}),$$

$$T_{m_1 m_2 m_3 m_4}^0 = \frac{1}{2} (\pi_{m_1 m_2 m_3 m_4} - \pi_{m_1 m_2 m_4 m_3}).$$

The total channel propagators (R_{λ} where $\lambda = \{d, m, s, t\}$) have to be found from the RPA-like matrix inversion:

$$\hat{R}_{\lambda}(i\omega) = [\hat{1} + \hat{R}_{\lambda}^0(i\omega) * U^{\lambda}]^{-1} * \hat{R}_{\lambda}^0(i\omega).$$

The derivation of the complete expression for the FLEX self-energy for the spin-polarized case with taking into account all the channels is rather cumbersome. Since we will not use here these complicated expressions, they will be discussed in detail elsewhere.⁴²

B. Hubbard-I approximation

Historically Hubbard-I approximation³³ was the first and the simplest approximation for a strongly correlated one-band model. It has, however, many inconsistencies (see, e.g., discussion in Ref. 41). For example, it is not conserving (the self-energy cannot be represented as a functional derivative of the generating functional with respect to the Green function) and therefore does not obey the Luttinger theorem and other ‘‘exact’’ Fermi-liquid properties. For the half-filled nondegenerate Hubbard model it always gives a gap in the energy spectrum, even for small U . This means that HIA is completely inapplicable for small and medium interactions. But at the same time it gives a correct picture of the electron spectrum in the narrow-band limit. Therefore it seems to be very useful in $4f$ systems with a very strong degree of localization of the electron states. Applying this to some real systems in the framework of the LDA++ approach, the HIA scheme could give (as will be shown below) an effective and nontrivial description of many-body multiplet effects.

To introduce Hubbard-I-type approximation in the degenerate case it is convenient to exploit the so-called atomic representation and Hubbard X operators (see Refs. 43, 1, and 44),

$$X_i^{\mu\nu} = |\mu\rangle \langle \nu|,$$

where μ, ν are multielectron states of the site i as a whole (configuration and multiplet indices). In terms of X operators the atomic Hamiltonian has a very simple form:

$$H^{\text{at}} = \sum_{\mu} E_{\mu} X^{\mu\mu}.$$

On the other hand, the intersite transfer Hamiltonian, which has very simple (bilinear) structure in terms of the

operators $c_{m'\sigma}^+$, $c_{m\sigma}$, also can be expressed in terms of X operators by the relations $c_{m\sigma} = \sum_{\mu\nu} \langle \mu | c_{m\sigma} | \nu \rangle X^{\nu\mu}$ and similarly for $c_{m'\sigma}^+$. In the limit of a very strong interaction it is convenient to calculate the Green function via X operators (using the decoupling procedure⁴⁴ or a special diagram technique for X operators⁴⁰) and then transform to electron operators. HIA corresponds to the following expression:^{33,44}

$$G^{-1}(i\omega) = [G^{\text{at}}(i\omega)]^{-1} - \hat{t}$$

where \hat{t} is the matrix of transfer integrals. In the limit of very small \hat{t} this expression describes the arising of separate bands from each intraatomic transition with the change of the electron number from unity. It is the picture that seems reasonable for, e.g., rare-earth materials with a very narrow $4f$ band. The bands always appear to be narrowed. Indeed, if in the vicinity of the pole $i\omega = \varepsilon_0$ the atomic Green function can be represented as

$$G^{\text{at}}(i\omega) = \frac{Z_0}{i\omega - \varepsilon_0};$$

the effective transfer Hamiltonian for this ‘‘Hubbard band’’ will be $Z_0\hat{t}$ instead of \hat{t} .

In terms of the LDA++ multiband approach HIA for the Green function has the following form:

$$G_{im,jm',\sigma}^{-1}(i\omega) = [(i\omega + \mu)\delta_{mm'} - \sum_{mm',\sigma}^{\text{at}}(i\omega)]\delta_{ij} - h_{mm',\sigma}^{ij}. \quad (8)$$

To obtain this Green function, we need to solve by an exact diagonalization (ED) technique the atomic many-electron problem:

$$H^{\text{at}}|v\rangle = E_v^{\text{at}}|v\rangle$$

with the effective atomic Hamiltonian for d or f states,

$$H^{\text{at}} = \sum_{mm',\sigma} \varepsilon_{mm'} c_{m\sigma}^+ c_{m'\sigma} + \frac{1}{2} \sum_{\{\sigma m\}} U_{m_1 m_2 m'_1 m'_2} c_{im_1\sigma}^+ c_{im_2\sigma}^+ c_{im'_2\sigma'} c_{im'_1\sigma'}; \quad (9)$$

here $\varepsilon_{mm'}$ is the matrix of atomic energies that in principle, can include nondiagonal terms. The latter naturally comes from the LMTO tight-binding effective Hamiltonian, which has a diagonal part of $h_{mm',\sigma}$ as a result of transformation to an orthogonal basis set.³⁵ Diagonalization of atomic Hamiltonian Eq. (9) is not a big problem for a standard work station, since it is equivalent to the five- and seven-site Hubbard model in the ED scheme³ for d and f states.

Using eigenfunctions and eigenvectors of the Hamiltonian [Eq. (9)], the exact atomic Green function can be found by the standard definition:²⁰

$$G_{mm',\sigma}^{\text{at}}(i\omega) = \frac{1}{Z} \sum_{\nu\mu} \frac{\langle \mu | c_{m\sigma} | \nu \rangle \langle \nu | c_{m'\sigma}^+ | \mu \rangle}{i\omega + E_\mu - E_\nu} (e^{-\beta E_\mu} + e^{-\beta E_\nu}), \quad (10)$$

where $Z = \sum_\nu e^{-\beta E_\nu}$.

Finally Σ^{at} , which is needed for HIA approximation, is found from the following expression:

$$\Sigma_{mm',\sigma}^{\text{at}}(i\omega) = i\omega \delta_{mm'} - \varepsilon_{mm'} - (G^{\text{at}})_{mm',\sigma}^{-1}(i\omega). \quad (11)$$

Now the HIA approach to LDA++ may be formulated as a functional for the atomic density matrix, $n_{mm'}$ with a constraint (for $\varepsilon_{mm'}$):

$$n_{mm'} = \frac{1}{\beta} \sum_\omega G_{mm',\sigma}^{\text{at}}(i\omega) + \frac{1}{2} \delta_{mm'} \quad (12)$$

(see Ref. 20) having the same $n_{mm'}$ density matrix for d or f electrons as in the crystal, as for the corresponding site and orbital element of the Green function, Eq. (8).

C. DMFT-multiband scheme

A great success of the dynamical mean-field ($d=\infty$) approach to the theory of correlated systems³ shows that probably this scheme can be the most accurate for the calculations of the self-energy from local description of electron fluctuations, at least in the vicinity of the metal-insulator transition. We will use this scheme for real crystals as a best local approximation. The DMFT scheme is based on the cavity method or the solution of the effective impurity problem, which corresponds to subtraction of the local self-energy only on the one atom in question. In Appendix A we show the equivalence of the cavity and impurity methods for matrix multiband Hamiltonians. It was realized recently that the success of DMFT in the one-band half-filled Hubbard model with simplest second-order self-energy is related to the fact that both small and large U limits are exact in this case.³ This is not true for the noninteger filling or for the multiband case. The elegant iterative perturbation IPS for noninteger one-band Hubbard model was proposed recently⁴⁵ and gives almost perfect agreement with ED and QMC results. For the case of a multiband with noninteger occupations the problem is much more severe and the existing IPS generalization⁴⁶ does not produce good results for large doping. Here we use the main idea of the original IPS method⁴⁵ and propose another version of multiband DMFT that is based more on the numerical solutions of corresponding atomic problem than the approximate analytical one used in Ref. 46.

The impurity problem for the ‘‘bath’’ Green function reads

$$[G_0(i\omega)]_{mm'}^{-1} = [G(i\omega)]_{mm'}^{-1} + (\mu_0 - \mu)\delta_{mm'} + \Sigma_{mm'}(i\omega),$$

where the local Green function is defined through Brillouin zone sum:

$$G_{mm'}(i\omega) = \frac{1}{N_k} \sum_{\mathbf{k}} G_{mm'}(\mathbf{k}, i\omega);$$

here N_k is the total number of \mathbf{k} points. Alternatively one may perform the \mathbf{k} integration using a complex-tetrahedron scheme.^{47,48} We introduce here according to Ref. 45 the ‘‘local’’ impurity chemical potential μ_0 to satisfy the condition

$$\sum_{\mathbf{k}} \int_{-\infty}^{+\infty} \frac{d\omega}{2\pi} \text{Tr} \left[\hat{G}(\mathbf{k}, i\omega) \frac{\partial \hat{\Sigma}(i\omega)}{\partial \omega} \right] = 0,$$

which is necessary to establish that the Luttinger theorem is true.

We use the following ansatz for the self energy is in the matrix (m, m') form:

$$\hat{\Sigma}(i\omega) = \hat{\Sigma}^{\text{HF}}(i\omega) + \hat{A} * \hat{\Sigma}^{(2)}(i\omega) * [\hat{1} - \hat{B}(i\omega) * \hat{\Sigma}^{(2)}(i\omega)]^{-1}, \quad (13)$$

where the second-order self-energy $\hat{\Sigma}^{(2)}(i\omega)$ is defined in terms of the bath Green function $\mathcal{G}_0(i\omega)$ in accordance with Eq. (5) with $W = V^{(2)}$ [see also Eq. (6)]:

$$\hat{\Sigma}^{(2)} = \hat{\Sigma}^{(2)}[\mathcal{G}_0].$$

In the spirit of the approach of Ref. 45 the A matrix should be defined to provide the exact high-energy ($\omega \rightarrow \infty$) limit of $\hat{\Sigma}(i\omega)$. The best way to bring about such an asymptotic is to use the equations of motion for the double-time retarded Green function with the analytical continuation on the Matsubara frequencies.^{20,40} One has an exact at $\omega \rightarrow \infty$ expression

$$\Sigma_{mm'\sigma}(i\omega) = \frac{1}{i\omega} N_{mm'\sigma},$$

where

$$N_{mm'\sigma} = \langle \{ [c_{m\sigma}, H_{\text{int}}], [H_{\text{int}}, c_{m'\sigma}^+] \} \rangle;$$

here $[\dots, \dots]$ and $\{\dots, \dots\}$ are the symbols for commutator and anticommutator, correspondingly, and H_{int} is the Hubbard (interaction) part of the Hamiltonian. Note that in the multiband case the average $N_{mm'\sigma}$ contains the products of four electron operators and cannot be found exactly. Decoupling of these four-fermion averages according to the Wick theorem and comparing the result with the asymptotic of $\hat{\Sigma}^{(2)}$,

$$\Sigma_{mm'\sigma}^{(2)}(i\omega \rightarrow \infty) = \frac{N_{mm'\sigma}^0}{i\omega},$$

we obtain the following expression:

$$\hat{A} = \hat{N} * [\hat{N}^0]^{-1},$$

where the \hat{N}_0 matrix defined in the spin-polarized case as

$$N_{mm'\sigma}^0 = \sum_{\{m_i\}} \left\{ U_{mm_3m_1m_4} U_{m_1m_5m'_2} \sum_{\sigma'} n_{m_5m_4\sigma'}^0 (\delta_{m_3m_2} - n_{m_3m_2\sigma'}) - U_{mm_3m_4m_1} U_{m_1m_5m'_2} n_{m_5m_4\sigma'}^0 (\delta_{m_3m_2} - n_{m_3m_2\sigma'}) \right\}$$

and in the nonmagnetic case it simplifies to

$$N_{mm'}^0 = \sum_{\{m_i\}} U_{mm_1m_3m_4}^d U_{m_1m_5m'_2} n_{m_5m_4}^0 (\delta_{m_3m_2} - n_{m_3m_2}^0).$$

The expression for the \hat{N} matrix differs from that for \hat{N}^0 by the replacement of the occupation matrix $n^0 \rightarrow n$. Note that matrix \hat{A} appears to be non-Hermitian. In the nondegenerate case this expression appears to be exact (see Ref. 45) due to the identity

$$(c_{m\sigma}^+ c_{m\sigma})^2 = c_{m\sigma}^+ c_{m\sigma}.$$

It can be quite accurate also in the general multiband case.

Coefficient matrix \hat{B} is designed to fix the exact atomic limit of the interaction self-energy, Eq. (13). There are other problems with coefficient B in the multiband case.⁴⁶ While in the single-band model one can find an analytical expression for the constant B ,⁴⁵ in the multiband case this parameter should be ω dependent, owing to the frequency dependence of the atomic self-energy, Eq. (11). We decide to find numerically the non-Hermitian matrix $B(i\omega)$ from the atomic limit of Eq. (13) using the exact $\hat{\Sigma}_{\text{at}}(i\omega)$ with a constraint for the density matrix \hat{n} . In this limit $\hat{\Sigma}^{(2)}(i\omega)$ in the nonmagnetic case has the form

$$\hat{\Sigma}_{mm'}^{(2)\text{at}}(i\omega) = \sum_{\{m_i\}} U_{mm_1m_3m_2}^d U_{m_1m_2m'_3} \times \frac{[f_{m_3}(1-f_{m_2}-f_{m_1}) + f_{m_1}f_{m_2}]}{i\omega + \mu_0 - \varepsilon_{m_2} + \varepsilon_{m_3} - \varepsilon_{m_1}};$$

here f_{m_i} and ε_{m_i} are diagonal occupation numbers and energies of h^{at} . In this case we have

$$\hat{B}(i\omega) = [\hat{\Sigma}^{(2)\text{at}}(i\omega)]^{-1} - [\hat{\Sigma}^{\text{at}}(i\omega) - \hat{\Sigma}^{\text{HF}}]^{-1} * \hat{A}. \quad (14)$$

As a simple example for such a scheme we compare in Fig. 1 the DMFT to exact diagonalization for the Anderson model of two sites, two bands with one correlated site $U = 4$, $\varepsilon_f = -4$ and one ‘‘free site’’ with $\varepsilon_0 = 0$ and hybridization between the sites $V = 0.25$.⁴⁶ For convenience we assume that all parameters for our model calculations are in eV energy units. The corresponding Hamiltonian for the Anderson impurity model has the following form:

$$H_{\text{imp}} = \varepsilon_f \sum_{m\sigma} f_{m\sigma}^+ f_{m\sigma} + V \sum_{m\sigma} (f_{m\sigma}^+ c_{m\sigma} + c_{m\sigma}^+ f_{m\sigma}) + U \sum_m f_{m\uparrow}^+ f_{m\downarrow} f_{m\downarrow}^+ f_{m\uparrow}.$$

It is not a problem to find an exact Green function for this model (the nonsymmetrized many-body Hamiltonian has the dimension 256×256) and compare it with approximate calculations. We see that the agreement between exact solution and our DMFT results is quite good even for a large filling ($n_{\text{tot}} > 1$; in this case $n_f = 0.76$, $n_{\text{tot}} \approx 2$). Also note that the atomic Green function in Fig. 1 for the correlated site has the three-peak structure for this occupation (there are, in general, eight poles in Green functions for the two-band case) and not the two-peak structure as in the one-band model. The use of the *numerical* atomic Green function for the $B(i\omega)$ -matrix

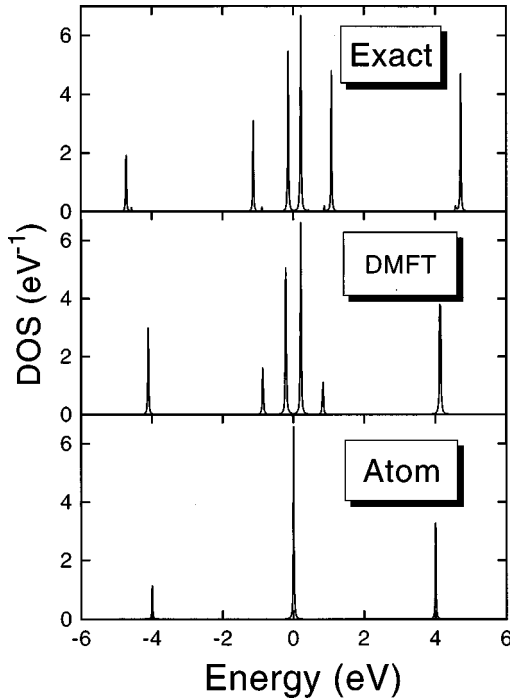


FIG. 1. Energy spectrum for two-band two-site Anderson model in exact diagonalization and DMFT scheme as well as atomic Green function for correlated site.

calculation is quite important even for qualitative agreement with exact results for such a model at a filling larger than one electron per site.⁴⁵

III. RESULTS FOR TWO-BAND MODEL

In this section we compare the three different LDA++ approaches described above for a two-band system. We used

$$\begin{aligned}
 U^d &= \begin{pmatrix} U+J & \delta J & \delta J & 2U-J \\ \delta J & 0 & 2J-U & \delta J \\ \delta J & 2J-U & 0 & \delta J \\ 2U-J & \delta J & \delta J & U+J \end{pmatrix}, & U^m &= \begin{pmatrix} -U-J & -\delta J & -\delta J & -J \\ -\delta J & 0 & -U & -\delta J \\ -\delta J & -U & 0 & -\delta J \\ -J & -\delta J & -\delta J & -U-J \end{pmatrix}, \\
 U^s &= \begin{pmatrix} U+J & \delta J & \delta J & 0 \\ \delta J & \frac{1}{2}(J+U) & \frac{1}{2}(J+U) & \delta J \\ \delta J & \frac{1}{2}(J+U) & \frac{1}{2}(J+U) & \delta J \\ 0 & \delta J & \delta J & U+J \end{pmatrix}, & U^t &= \begin{pmatrix} 0 & 0 & 0 & 0 \\ 0 & \frac{1}{2}(J-U) & \frac{1}{2}(J-U) & 0 \\ 0 & \frac{1}{2}(J-U) & \frac{1}{2}(J-U) & 0 \\ 0 & 0 & 0 & 0 \end{pmatrix}.
 \end{aligned}$$

We investigate this model for different U parameters: $U = 2-8$ with the fixed values of $J=0.5$ and $\delta J=0.1$. The total number of electrons is $n_{\text{tot}}=1.4$, which approximately corresponds to fully occupied z bands and the almost half-filled x band with 10% holes. We use the 32×32 mesh for the summation over the Brillouin zone and the 4000–8000 Matsubara frequencies with the cutoff energy equal to 20–40 times the bandwidth. In Fig. 2 we show the results of

the simplified two-dimensional model for high- T_c superconductors for $d_{x^2-y^2} \equiv x$ and $d_{z^2} \equiv z$ orbitals.³⁴ If one can skip the z orbital it will be the standard single-band nearest-neighbor hopping t model. The LDA band-structure calculation for high- T_c materials shows the large contribution of Cu d_{z^2} orbital to states near the Fermi level.⁴⁹ Therefore the situation with two correlated valence bands could be possible in this materials. Although we knew that for the realistic description of the Cu $d_{x^2-y^2}$ state in the single-band model one need to include next-nearest hoppings (coming from interactions with O $2p$ - and Cu $4s$ orbitals⁴⁹) we used here the simplified tight-binding (TB) model for two correlated bands x and z within the nearest-neighbor hopping approximation. The one-electron Hamiltonian has the following form:³⁴

$$\hat{h}(\mathbf{k}) = \begin{pmatrix} -2t_{xx}(\cos k_x + \cos k_y) + \Delta, & -2t_{xz}(\cos k_x - \cos k_y) \\ -2t_{xz}(\cos k_x - \cos k_y), & -2t_{zz}(\cos k_x + \cos k_y) \end{pmatrix}.$$

The hopping parameters are related via a simple Slater-Koster ratio: $t_{xx}=1$, $t_{zz}=0.3$, $t_{xz}=0.4$. Again we assume that all TB parameters are in eV energy units, while the value $t_{xx} \sim 0.5$ eV would be more realistic.⁴⁹ It is important to take into account the energy shifting parameter Δ since Cu $d_{x^2-y^2}$ bands are located higher than the Cu d_{z^2} one, so we use $\Delta = 4$. For the Coulomb energy our parameterization corresponds to the following matrix elements ($m_1 \neq m_2$): $U_{m_1 m_1 m_1 m_1} = U + J$, $U_{m_1 m_2 m_1 m_2} = U$, $U_{m_1 m_2 m_2 m_1} = J$, and $U_{m_1 m_2 m_1 m_1} = \delta J$. In this case the symmetrized bare vertices has the following form (the basis function numbering as xx, xz, zx, zz):

self-consistent FLEX two-band calculations for $U=2, 4, 6$, and 8. The density of states (DOS) was obtained from the Green function, extrapolating Matsubara frequencies with the Pade approximation⁵⁰ to the real axis. Note that the bare bandwidth for $t_{xz}=0$ is equal to $8t$ in the case of two-dimensional square lattice and corresponds to 8 and 2.4 eV for x and z bands. One can see the narrowing of the DOS peak near the Fermi energy (E_F) for the x band and the

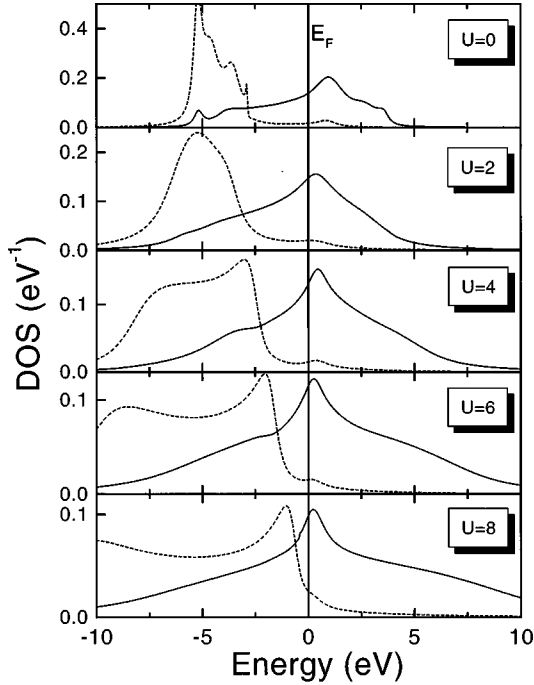


FIG. 2. Density of states for the two-band model in the FLEX scheme for different U values. Full and dashed lines indicate partial DOS for x and z orbitals.

boarding of the total x and z -subbands as U increased. An interesting feature of this two-band model is seen in moving the peak from occupied z bands towards the Fermi level with increasing correlation strength U , and a pinning of the van Hove peak from the x band just above Fermi level. This drastic change of the x and z band shape maximizes the particle-hole interband susceptibility (inversely proportional to the energy distance between band peaks) and therefore increases the fluctuation contribution to FLEX energy. The value of the average inverse mass enhancement factor $Z = [1 - \partial \Sigma(\epsilon) / \partial \epsilon]_{\epsilon=0}^{-1}$ is equal to 0.45 and 0.83 for x and z orbitals for $U=4$. Spectral function $A(\mathbf{k}, \epsilon) = -1/\pi \text{Tr} \text{Im} G(\mathbf{k}, \epsilon)$ for three different \mathbf{k} directions in the two-dimensional Brillouin zone is shown in Fig. 3. One could see the renormalized dispersion of two bands: the x band from approximately -5 eV at the X point to 5 eV at the M point and the z band from approximately -8 eV at the X point to 3 eV at the M point. Similar to all high- T_c models³⁶ there is an extended van Hove singularity in x bands just at the Fermi energy near the X point.

The results of self-consistent DMFT calculations for $U=4$ and 8 are presents in Fig. 4. In this case we use only first seven Matsubara frequencies in Eq. (14) and the constant B matrix for the rest frequencies. One can clearly see some differences to the corresponding FLEX results, which are related to a sharpness of the DOS near E_F and the more pronounced three-peak structure of the partial x -band DOS for $U=8$. We plot also the DOS corresponding to the atomic Green function for $U=8$ with the four poles near the Fermi energy out of eight poles in the paramagnetic two-orbital atom. The corresponding spectral function for the same directions in the Brillouin zone is present in Fig. 5 for $U=8$. There is a sharp quasiparticle dispersion near the Fermi level and a broad incoherent background above E_F at an energy of

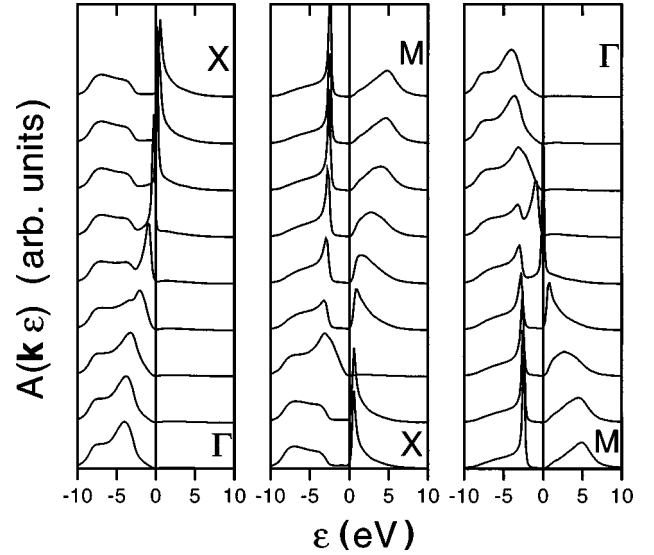


FIG. 3. Spectral function (the two-band FLEX model, $U=4$) for three different directions in the two-dimensional square Brillouin zone: $\Gamma=(0,0)$, $X=(0.5,0)$, and $M=(0.5,0.5)$ in units of $2\pi/a$.

about 7 eV near the M point. An extended van Hove singularity at the X point becomes more pronounced. We plot also the momentum distribution function $n(\mathbf{k})$ in $(1,1)$ direction in the Fig. 6. From the quasiparticle dispersion of the x band along the Γ - M direction (Fig. 5), we expect the Fermi surface crossing almost exactly halfway between these two points. The momentum distribution function (Fig. 6) just confirms this situation and shows that the Fermi step (our simulation temperature $T=0.06t$) is smaller than 1 and

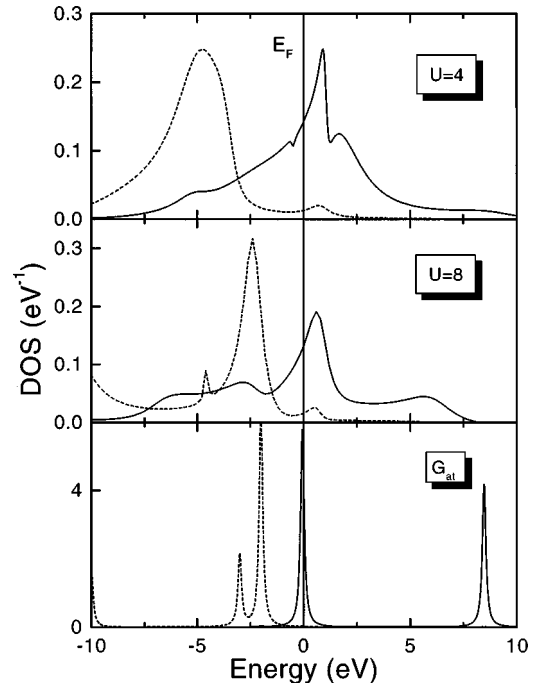


FIG. 4. Density of states for the two-band model in the DMFT scheme for different U values as well as the atomic Green function for $U=8$. Full and dashed lines indicate partial DOS for x and z orbitals.

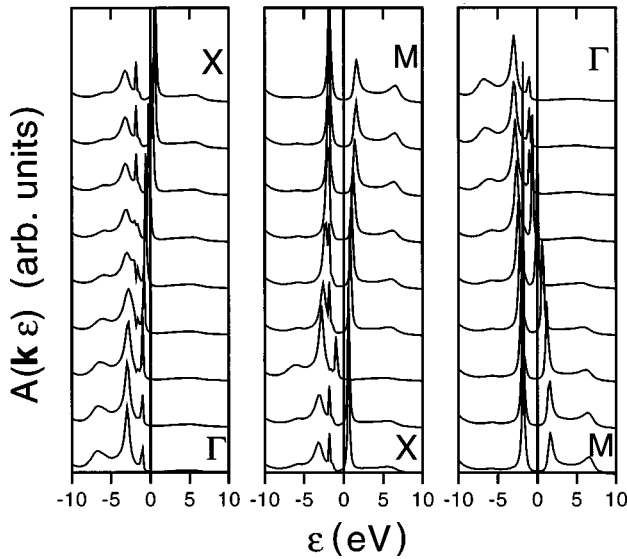


FIG. 5. Spectral function (the two-band DMFT model $U=8$) for three different directions in the two-dimensional square Brillouin zone.

agrees with the calculated value of the mass renormalization factor $Z=0.43$ for the x band.

Finally, the HIA solution for this two-band model for $U=8$ is shown in Fig. 7. In this case we have the dielectric DOS with narrow atomiclike resonances. It is interesting to note that the structure of the atomic Green function in the DMFT approximation (Fig. 4) quite close to the HIA solution shifted down by approximately 2 eV. We would like to mention that the application of the HIA scheme is reasonable only for $U \gg W$ and not for $U=W$ as in this case.

IV. LDA++ CALCULATIONS FOR REAL SYSTEMS

The self-consistent LDA++ calculation for real systems pose a serious computational problem. One needs to operate with the susceptibility matrix, which is of dimension $N_d^2 \times N_d^2$ and depends on the Matsubara frequencies. For an illustrative purpose we have calculated the electronic structure of classical Mott-Hubbard insulator NiO and mixed-valence $4f$ -compound TmSe in the HIA scheme for LDA++. We use the non-self-consistent HIA approximation with the sim-

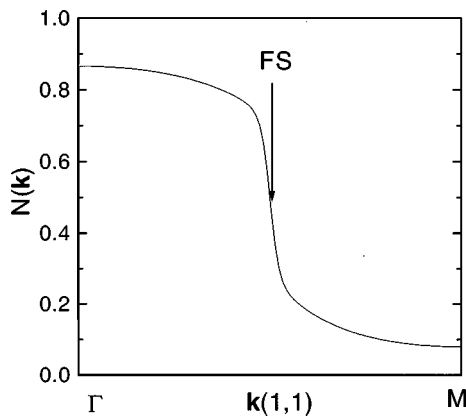


FIG. 6. The momentum distribution function $n(\mathbf{k})$ in the (1,1) direction for the two-band DMFT model $U=8$.

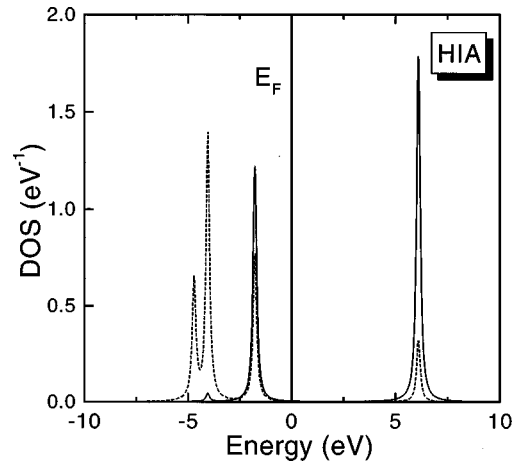


FIG. 7. Density of states for the two-band model in the HIA scheme for $U=8$. Full and dashed lines indicate partial DOS for x and z orbitals.

plest constraint for only diagonal ε_f in Eq. (9) to have n_d for NiO or n_f electrons for TmSe from self-consistent paramagnetic LDA calculations. The Coulomb matrix is expressed via effective Slater integrals:

$$U_{m_1 m_2 m'_1 m'_2} = \sum_k a_k(m_1, m'_1, m_2, m'_2) F^k,$$

where $0 \leq k \leq 2l$ and

$$a_k(m_1, m'_1, m_2, m'_2) = \frac{4\pi}{2k+1} \sum_{q=-k}^k \langle l m_1 | Y_{kq} | l m'_1 \rangle \times \langle l m_2 | Y_{kq}^* | l m'_2 \rangle.$$

We used the following effective Slater parameters, which define screened Coulomb interaction in the d shell for NiO: $F^0=8.0$ eV, $F^2=8.2$ eV, and $F^4=5.2$ eV, and in the f shell for TmSe: $F^0=5.7$ eV, $F^2=9.1$ eV, $F^4=5.7$ eV, and $F^6=4.7$ eV (see, e.g., Refs. 16, 51, and 52). We start from the nonmagnetic LDA calculations in the LMTO nearly orthogonal representation³⁵ for experimental crystal structures of NiO and TmSe. The minimal basis set of s , p , and d orbitals for NiO and s , p , d , and f orbitals for TmSe corresponds to the 18×18 and 32×32 matrices of the LDA Hamiltonian $h(\mathbf{k})$. The occupation number for correlated electrons are 8.4 electrons in the d shell of Ni and 12.6 electrons in the $4f$ shell of Tm. Using the corresponding atomic self-energy for the Ni atom and Tm atom the total DOS's for NiO and TmSe have been calculated from Eq. (8). In Fig. 8 we compare the paramagnetic LDA results with the HIA LDA++ scheme. It is well known that the paramagnetic LDA calculations cannot produce the insulating gap in nickel oxide: the Fermi level located in the middle of the half-filled e_g bands.¹⁸ In the HIA approximation to the LDA++ approach there is a gap (or pseudogap in Fig. 8 due to temperature broadening) of the order of 3.5 eV even in this nonmagnetic state. This gap and the satellites at -5 and -8 eV are related to the structure of the atomic Green function shown in the lower panel of Fig. 8.

In Fig. 9 we compare the calculated DOS for TmSe with experimental x-ray photoemission spectroscopy.⁵³ The HIA

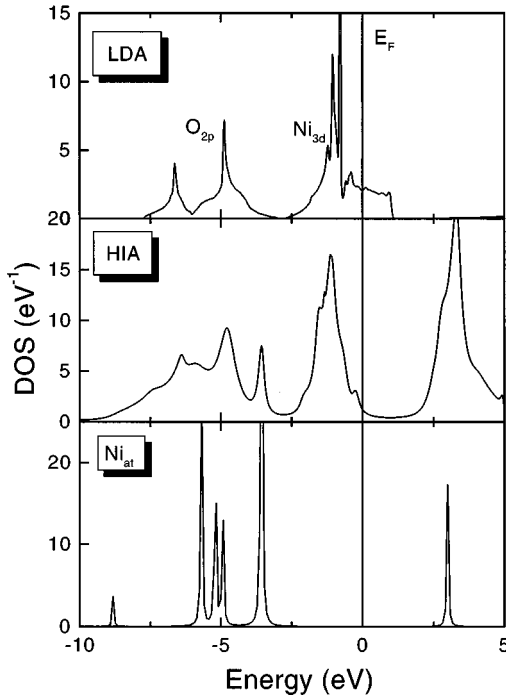


FIG. 8. Density of states for paramagnetic nickel oxide in the LDA and HIA approximations as well as the Ni-atom Green function.

approximation in this case well reproduces the ladder-type photoemission spectrum, comes mainly from combinations of two multiplets structure of $Tm^{2+}(f^{13})$ and $Tm^{3+}(f^{12})$. This example demonstrates how the LDA++ scheme can combine the many-body atomic physics with band structure methods. The normal LDA-band structure for rare-earth sys-

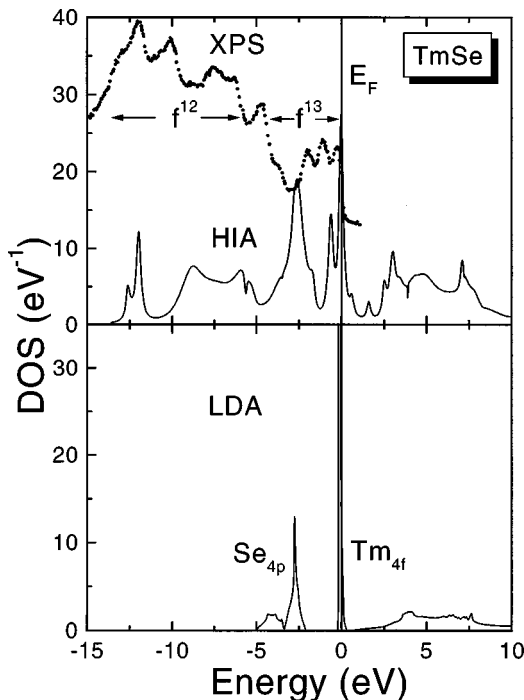


FIG. 9. Density of states for TmSe in the HIA scheme in comparison with the experimental XPS spectrum (Ref. 53) and the results of paramagnetic LDA calculations.

tems corresponds to the narrow f peak at the Fermi level and could not describe the experimental XPS spectrum, which has the f resonances over a wide energy range of the order of 12 eV. At the same time, HIA is not adequate to describe correctly the fine features of the electron structure near the Fermi level. It is known⁵⁴ that TmSe is really the narrow-gap semiconductor. According to the most developed model approach to mixed-valence semiconductors^{55,1} the appearance of this energy gap is caused by both hybridization and excitation effects due to the Coulomb attraction of the $5d$ conduction electron and $4f$ hole. This effect cannot be described in the HIA approximation. Nevertheless, we believe that the description of the electronic structure of f compounds including mixed-valence ones on the large energy scales is important in and of itself and in this sense the results presented here demonstrate the usefulness of the LDA++ approach for the description of real strongly correlated systems.

V. SUMMARY

We have formulated a general LDA++ scheme that takes into account dynamical electron fluctuations in the case of correlated d or f states. The most accurate approach is the DMFT-band structure method, while the more simple FLEX and HIA schemes can be useful as well for investigation of correlation effects in real systems, in the cases of rather weak and rather strong interaction, respectively. In principle, one could combine the idea of the bath Green function in the DMFT scheme with the simple expression for the self-energy in the FLEX approximation. In this case $\hat{\Sigma} = \hat{\Sigma}^{\text{FLEX}}[\mathcal{G}_0]$, and we expected to effectively reduce the effects of vertex corrections in the FLEX scheme.

Here we compare the LDA++ approach with more simple LDA+ U one. First of all, to describe Mott insulators in the LDA+ U approach (as well as in the SIC approach) it is necessary to assume magnetic and (or) orbital ordering.¹⁸ In LDA++ it is possible to consider the *paramagnetic* Mott insulators in the framework of *ab initio* calculations. Moreover, it is possible to obtain not only the Mott-Hubbard gap in the electron spectrum but also satellites and multiplet structure (see, e.g., the results for TmSe and NiO in the previous section).

The correlation effects results from the frequency dependence of the self-energy (the non-Fermi-step form of the distribution function for quasiparticles, the mass enhancement, the appearance of many-electron Kondo resonances, etc.) can be obtained and investigated in the LDA++ approach but not in the LDA+ U . Our results for the two-band model provide interesting examples of such behavior. In particular, it is worthwhile to note such features as the narrowing of the van Hove singularity and its “pinning” to the Fermi level (which is important for the physics of high T_c superconductors³⁶ and can be described already in the multiband FLEX approximation), the three-peak structure of the spectrum in the vicinity of Mott insulators (Kondo resonance and midgap states that can be described in the DMFT approach).

We hope that the approximations described here may be useful for the *ab initio* calculations of the electron structure of a great variety of strongly correlated electron systems including doped Mott insulators, rare-earth metals, and their compounds (in particular mixed-valence ones), high-

temperature superconductors, and many others.

ACKNOWLEDGMENTS

Part of this work was carried out during the visit of one author (M.I.K.) to the Max-Planck-Institute of Solid State (Stuttgart), Max-Planck-Institute of Physics of Complex Systems (Dresden), and Forschungszentrum Jülich. The authors are grateful to the Max-Planck Society and Forschungszentrum Jülich and benefited greatly from discussions with O.K. Andersen, V.I. Anisimov, A.O. Anokhin, P. Fulde, O. Gunnarsson, L. Hedin, P. Horsh, and G. Kotliar.

APPENDIX A

Here we present the proof of the equivalence of a cavity method and impurity problem in DMFT for the multiband case. We start with the expression for the Green-function matrix on the zero site in the cavity method [see Ref. 3, Eq. (35)],

$$[\mathcal{G}_0(i\omega)]^{-1} = i\omega + \mu - h_{\text{at}} - R,$$

where

$$R = \sum_{ij} t_{0i} G_{ij}^{(0)} t_{j0} \quad (\text{A1})$$

with h_{at} being the one-electron part of the intra-atomic Hamiltonian. All of these functions are the matrix in (m, m') indices as well as the diagonal matrix in spin space. Note that $G_{ij}^{(0)}$ is the Green function between sites i and j on the lattice with the site zero being eliminated,

$$G_{ij}^{(0)} = G_{ij} - G_{i0} G_{00}^{-1} G_{0j}. \quad (\text{A2})$$

Using the Fourier expansion of all the quantities over the Brillouin zone and substituting Eq. (A2) to Eq. (A1) one has

$$R = M - L G_{00}^{-1} L^T,$$

where

$$L = \sum_i t_{0i} G_{i0} = \sum_{\mathbf{k}} t(\mathbf{k}) G(\mathbf{k})$$

and

$$M = \sum_{ij} t_{0i} G_{ij} t_{j0} = \sum_{\mathbf{k}} t(\mathbf{k}) G(\mathbf{k}) t(\mathbf{k}).$$

At the same time (see Ref. 3)

$$G(\mathbf{k}) = [\Lambda - t(\mathbf{k})]^{-1},$$

$$\Lambda = i\omega + \mu - h_{\text{at}} - \Sigma(i\omega). \quad (\text{A3})$$

Taking into account that $\sum_{\mathbf{k}} t(\mathbf{k}) = 0$ one obtains

$$L = \sum_{\mathbf{k}} [t(\mathbf{k}) - \Lambda + \Lambda][\Lambda - t(\mathbf{k})]^{-1} = -1 + \Lambda G_{00}$$

and

$$L^T = -1 + G_{00} \Lambda.$$

One can obtain by the similar way the result for M matrix: $M = \Lambda L^T$.

Substituting all of these formulas into Eq. (A1) we have

$$R = (\Lambda + G_{00}^{-1} - \Lambda) L^T = -G_{00}^{-1} + \Lambda.$$

Using Eq. (A3), we can finally write

$$[\mathcal{G}_0(i\omega)]^{-1} = i\omega + \mu - h_{\text{at}} - \Lambda + G_{00}^{-1} = \Sigma(i\omega) + G_{00}^{-1}.$$

It means that $\mathcal{G}_0(i\omega)$ is the Green function of the impurity problem with the on-site one-electron Hamiltonian $h_{\text{at}} + \Sigma(i\omega)$ on each nonzero site and h_{at} for the zero site.

- ¹S.V. Vonsovskii, M.I. Katsnelson, and A.V. Trefilov, Phys. Met. Metallogr. **76**, 247,343 (1994).
- ²P.W. Anderson, *50 Years of the Mott Phenomenon*, in Frontiers and Borderlines in Many Particle Physics, edited by J.R. Schrieffer and R.A. Broglia (North-Holland, Amsterdam, 1988).
- ³A. Georges, G. Kotliar, W. Krauth, and M. Rozenberg, Rev. Mod. Phys. **68**, 13 (1996).
- ⁴D.J. Scalapino, Phys. Rep. **251**, 1 (1994).
- ⁵P. Hohenberg and W. Kohn, Phys. Rev. **136**, B864 (1964).
- ⁶R.O. Jones and O. Gunnarsson, Rev. Mod. Phys. **61**, 689 (1989).
- ⁷E.K.U. Gross and W. Kohn, Phys. Rev. Lett. **55**, 2850 (1985); M. Petersilka, U.J. Gossmann, and E.K.U. Gross, *ibid.* **76**, 1212 (1996).
- ⁸A. Flesar, A.A. Quong, and A.G. Eguiluz, Phys. Rev. Lett. **74**, 590 (1995).
- ⁹L. Mitás and R. Martin, Phys. Rev. Lett. **72**, 2438 (1994).
- ¹⁰S. Tanaka, J. Phys. Soc. Jpn. **64**, 4270 (1995).
- ¹¹R.Q. Hood, M.Y. Chou, A.J. Williamson, G. Rajagopal, R.J. Needs, and W.M.C. Foulkes, Phys. Rev. Lett. **78**, 3350 (1997).
- ¹²L. Hedin, Phys. Rev. **139**, A796 (1965).
- ¹³F. Aryasetiawan and O. Gunnarsson, Phys. Rev. Lett. **74**, 3221 (1995).

- ¹⁴A. Seidl, A. Görling, P. Vogl, J.A. Majewski, and M. Levy, Phys. Rev. B **53**, 3764 (1996); H. Rücker (unpublished).
- ¹⁵G.E. Engel, Phys. Rev. Lett. **78**, 3515 (1997).
- ¹⁶V.I. Anisimov, J. Zaanen, and O.K. Andersen, Phys. Rev. B **44**, 943 (1991).
- ¹⁷V.I. Anisimov, I.V. Solov'yev, M.A. Korotin, M.T. Czyzyk, and G.A. Sawatzky, Phys. Rev. B **48**, 16 929 (1993).
- ¹⁸V.I. Anisimov, F. Aryasetiawan, and A.I. Lichtenstein, J. Phys.: Condens. Matter **9**, 767 (1997).
- ¹⁹A. Svane and O. Gunnarsson, Phys. Rev. Lett. **65**, 1148 (1990).
- ²⁰A.A. Abrikosov, L.P. Gorkov, and I.E. Dzialoshinskii, *Methods of Quantum Field Theory in Statistical Physics* (Pergamon, New York, 1965).
- ²¹G. Mahan, *Many-Particle Physics* (Plenum, New York, 1981).
- ²²A.I. Lichtenstein and M.I. Katsnelson, Bull. Am. Phys. Soc. **42**, 573 (1997).
- ²³L. Kleinman and K. Mednick, Phys. Rev. B **24**, 6880 (1981).
- ²⁴G. Tréglia, F. Ducastelle, and D. Spanjaard, J. Phys. (Paris) **43**, 341 (1982).
- ²⁵M.M. Steiner, R.C. Albers, and L.J. Sham, Phys. Rev. B **45**, 13 272 (1992).

- ²⁶M.M. Steiner, R.C. Albers, and L.J. Sham, Phys. Rev. Lett. **72**, 2923 (1994).
- ²⁷I.S. Sandalov, O. Hjortstam, B. Johansson, and O. Eriksson, Phys. Rev. B **51**, 13 987 (1995).
- ²⁸F. Manghi, C. Calandra, and S. Ossicini, Phys. Rev. Lett. **73**, 3129 (1994).
- ²⁹M. Takahashi and J. Igarashi, Phys. Rev. B **54**, 13 566 (1996).
- ³⁰F. López-Aguilar, J. Costa-Quintana, and L. Puig-Puig, Phys. Rev. B **48**, 1128 (1993); **48**, 1139 (1993); **54**, 10 265 (1996).
- ³¹J.E. Han, M. Alouani, and D.L. Cox, Phys. Rev. Lett. **78**, 939 (1997).
- ³²N.E. Bickers and D.J. Scalapino, Ann. Phys. (N.Y.) **193**, 206 (1989).
- ³³J. Hubbard, Proc. R. Soc. London, Ser. A **276**, 238 (1963); **277**, 237 (1964).
- ³⁴F. Buda, D.L. Cox, and M. Jarrell, Phys. Rev. B **49**, 1255 (1994).
- ³⁵O.K. Andersen, O. Jepsen, and G. Krier, in *Lectures on Methods of Electronic Structure Calculations*, edited by V. Kumar, O.K. Andersen, and A. Mookerjee (World Scientific, Singapore, 1994), p. 63.
- ³⁶A.I. Liechtenstein, O. Gunnarsson, O.K. Andersen, and R.M. Martin, Phys. Rev. B **54**, 12 505 (1996).
- ³⁷R. Putz, R. Preuss, A. Muramatsu, and W. Hanke, Phys. Rev. B **53**, 5133 (1996).
- ³⁸A.I. Liechtenstein, V.I. Anisimov, and J. Zaanen, Phys. Rev. B **52**, R5467 (1995).
- ³⁹J.W. Serene *et al.* Phys. Rev. B **44**, 3391 (1991).
- ⁴⁰Yu.A. Izyumov, M.I. Katsnelson, and Yu.N. Skryabin, *Magnetism of Itinerant Electrons* (Nauka, Moscow, 1994).
- ⁴¹F. Gebhard, *The Mott Metal-Insulator Transition* (Springer, Berlin, 1997).
- ⁴²M.I. Katsnelson and A.I. Lichtenstein (unpublished).
- ⁴³J. Hubbard, Proc. R. Soc. London, Ser. A **285**, 542 (1965).
- ⁴⁴V.Yu. Irkhin and Yu.P. Irkhin, Phys. Status Solidi B **183**, 9 (1994).
- ⁴⁵H. Kajueter and G. Kotliar, Phys. Rev. Lett. **77**, 131 (1996); H. Kajueter, Ph.D. thesis, Rutgers University, 1996.
- ⁴⁶H. Kajueter and G. Kotliar, Int. J. Mod. Phys. B **11**, 729 (1997).
- ⁴⁷Ph. Lambin and J.P. Vigneron, Phys. Rev. B **29**, 3430 (1984).
- ⁴⁸V.I. Anisimov, A.P. Poteryaev, M.A. Korotin, A.O. Anokhin, and G. Kotliar, J. Phys. Condens. Matter **9**, 7359 (1997).
- ⁴⁹O.K. Andersen, A.I. Lichtenstein, O. Jepsen, and F. Paulsen, J. Phys. Chem. Solids **56**, 1573 (1995).
- ⁵⁰H.J. Vidberg and J.W. Serene, J. Low Temp. Phys. **29**, 179 (1977).
- ⁵¹D. van der Marel and G.A. Sawatzky, Phys. Rev. B **37**, 10 674 (1988).
- ⁵²B.L. Thole, G. van der Laan, J.C. Fuggle, G. A. Sawatzky, R. Karnatak, and J. Esteva, Phys. Rev. B **32**, 5107 (1988).
- ⁵³M. Campagna, G.K. Wertheim, and E. Bucher, *Structure and Bonding* (Springer, New York, 1976), Vol. 30, p. 99.
- ⁵⁴P. Wachter, J. Magn. Magn. Mater. **31-34**, 439 (1985); A. Amato and J. Sierro, *ibid.* **47-48**, 475 (1985).
- ⁵⁵V.Yu. Irkhin and M.I. Katsnelson, Zh. Éksp. Teor. Fiz. **90**, 1080 (1986) [Sov. Phys. JETP **63**, 631 (1986)]; Fiz. Tverd. Tela **29**, 1461 (1987) [Sov. Phys. Solid State **29**, 835 (1987)].